PERGAMON

Chemical Engineering Science 56 (2001) 2967–2977

Chemical Engineering Science

www.elsevier.nl/locate/ces

Microstructure evolution and rheological responses of hard sphere suspensions

Jae-Hyun So[a], Seung-Man Yang[a,*], Jae Chun Hyun[b]

[a]*Department of Chemical Engineering, Korea Advanced Institute of Science and Technology, 373-1, Kusong-dong, Yusung-ku, Taejon, 305-701, South Korea*
[b]*Department of Chemical Engineering, Korea University, Seoul, 136-701, South Korea*

Received 4 May 2000; received in revised form 1 August 2000; accepted 22 August 2000

Abstract

In the present study, the microstructural transitions of concentrated 'hard-sphere' suspensions under a simple shear flow were investigated by measuring the shear viscosity and flow-induced dichroism. Monodisperse silica particles of two different sizes, 260 and 545 nm in diameter, were prepared by the so-called modified Stöber method. The monodisperse particles were coated with 3-(trimethoxysilyl)propyl methacrylate (MPTS) to enhance the dispersion stability at high particle volume fractions (ϕ) up to $\phi = 0.55$. The particles were dispersed in a refractive-index matching solvent, tetrahydrofurfuryl alcohol, in which the van der Waals dispersion forces were diminished. The smaller particle suspension exhibited a smooth shear thinning up to $\phi = 0.55$ within our shear rate window, independently of the surface modification with the silane coupling agent MPTS. Meanwhile, for the larger silica particle suspension, the viscosity shear thinned at low shear rates and shear thickened at high shear rates when ϕ exceeded about 0.5. The surface modification enhanced its dispersion stability and slightly decreased the shear viscosity. Finally, the flow-induced dichroism from light passed in the flow-gradient direction probed the order–disorder transition effectively for the larger particle suspensions, such as disappearance of hexagonally ordered layered structure and formation of particle clustering. © 2001 Published by Elsevier Science Ltd.

Keywords: Suspension; Rheology; Microstructure; Dispersion; Hard spheres; Order–disorder transition

1. Introduction

The flow of particle dispersions has been studied intensively owing to its practical significance in paints, polymers, ceramics, composite materials, electronic industry, coating process and so on. Generally, particle dispersion shows high non-Newtonian behaviour even though the medium is a Newtonian liquid. And the deviation from the Newtonian flow behaviour becomes pronounced at high particle volume fractions and under strong flow field. When the imposed flow becomes strong, concentrated suspensions often show gradual or abrupt increase in the shear viscosity. Continuous or discontinuous shear thickening affects actual process or deceases productivity (Barnes, 1989; Barnes, Hutton, & Walters, 1989). Therefore, it is necessary to investigate the microstructural changes in the suspension under flow field. By doing so, we can understand the flow characteristics of concentrated particle suspensions and somehow prevent severe fracture problems in practical processes.

During last few decades, a number of studies have been done by rheometry (Krieger & Dougherty, 1959; Hoffman, 1972, 1974; de Kruif, van Iersel, Vrij, & Russel, 1985; Choi & Krieger, 1986; van der Werff & de Kruif, 1989; Boersma, Baets, Laven, & Stein, 1990a,b; Bender & Wagner, 1996; Fagan & Zukoski, 1997), by computer simulations (Bossis & Brady, 1989; Brady, 1993; Brady & Morris, 1997; Foss & Brady, 2000; Catherall, Melrose, & Ball, 2000) and by scattering methods (Laun et al., 1992; Chow & Zukoski, 1995a,b; Bender & Wagner, 1995). The rheological behaviour of a dilute particle dispersion was pioneered theoretically by Einstein (Furth & Cowper, 1956) and thereafter, the applicable range of particle loading was extended to a semi-dilute suspension by several researchers (Batchelor, 1977; Russel & Gast, 1986). For example, Batchelor (1977), Russel and Gast (1986), Bossis and Brady (1989), Foss and Brady (2000), Brady (1993) and Brady and Morris (1997), predicted

* Corresponding author.
E-mail address: smyang@kaist.ac.kr (S.-M. Yang).

0009-2509/01/$ - see front matter © 2001 Published by Elsevier Science Ltd.
PII: S0009-2509(00)00474-7

theoretically the macroscopic properties of particle suspensions by considering the particle–particle interactions either from the statistical mechanics point of view or by 'Stokesian dynamics' simulation.

In general, monodisperse hard sphere suspension begins to order into a macrocrystalline structure of face centered cubic (FCC) or hexagonally close packing (HCP), when the particle volume fraction (ϕ) exceeds 0.5 under equilibrium condition with no imposed flow. Further, when $0.5 < \phi < 0.55$, the random disordered phase and the colloidal crystalline phase coexist (Russel, Saville, & Schowalter, 1989; Gast & Russel, 1998; Larson, 1999). When $\phi > 0.55$, the formation of FCC or HCP structure is completed in the suspension. The structural transition is due to the fact that the particles gain entropy by arranging themselves equidistantly from one another to maximize the space in their vicinity. The severe shear thinning observed at high concentrations arises from three-dimensionally ordered structures of FCC or HCP. When ordered phases are forced to flow, one typically observes a yield stress above which the macrocrystal orients so that the direction of closest packing of the spheres is aligned to flow velocity, while the planes containing the closest packings are parallel to the shearing surfaces (Ackerson, 1990; Chow & Zukoski, 1995a,b). Thus, at low shear rates, the three-dimensional ordered structure transforms into a two-dimensionally layered structure that permits continuous deformation. Then, the viscosity drops drastically. At high shear rates, however, the enhanced hydrodynamic force prevents them from sustaining their ordered state by forming three-dimensional network or clustering. Bossis and Brady (1989) showed explicit evidence that the cluster size grows as the shear rate is increased, and suggested that the particle clustering is the origin of shear thickening. Moreover, a recent theoretical work by Brady and Morris (1997) provides a prediction on the origin and the onset shear rate at which shear thickening occurs.

Meanwhile, as the volume fraction increases, a particle approaches its nearby particles closer, and consequently tremendous lubrication stress develops (Graham, Steele, & Bird, 1984). Further, considerable amount of the solvent is trapped in the interior of the particle cluster, which is formed by the strong hydrodynamic force. The entrapping of the solvent apparently decreases the mobile solvent volume fraction, or in effect, increases the particle volume fraction. For example, if the particle clustering forms a dimer or trimer, the effective particle volume fraction increases 5/4 and 4/3 times, respectively, due to the immobilized volume effect (Graham et al., 1984). The cluster formation and the resulting high lubrication stress in the concentrated suspension are responsible for the sudden and substantial increase of the shear viscosity and stress.

Recently, Foss and Brady (2000) reported non-equilibrium behaviour of concentrated Brownian hard sphere dispersions with volume fractions (ϕ) ranging from 0.316 to 0.49. For these suspensions, they showed that there was no ordering of ideal hard sphere suspensions under shear flow. On the other hand, when dispersed particles are electrostatically stabilized and experience sufficiently long-ranged and strong interparticle repulsions, hexagonally packed string ordering occurs before the onset of shear thickening. This coincides well with experimental observations (Ackerson, 1990; Chen, Ackerson, & Zukoski, 1994). Moreover, Catherall et al. (2000) performed Stokesian simulation for shear thickening and order–disorder transitions in surface-charge stabilized suspensions, electrosterically stabilized suspensions with coated polyelectrolyte layer, and sterically stabilized suspensions with coated polymer layer. For the sterically stabilized suspensions, no ordering was observed with the core volume fraction of 0.42, while ordering was observed with $\phi = 0.54$ although no drastic thickening was observed. However, the microstructure evolutions and related rheological behaviour of *highly* concentrated hard sphere suspensions have not been successfully explained yet especially in terms of the effects of stabilization of the particle dispersions, which is of practical significance.

In the present work, the rheological behaviour and phase stability were investigated for highly concentrated hard sphere silica suspensions. Monodisperse silica particles have been synthesized successfully through sol–gel method (Stöber, Fink, & Bohn, 1968; van Helden, Jansen, & Vrij, 1981; Bogush, Tracy, & Zukoski, 1988; Philipse & Vrij, 1989; Lee & Yang, 1997; Lee & Yang, 1998a,b; Lee, So, & Yang, 1999; Oh, So, Lee, & Yang, 1999a,b). In particular, van Helden et al. (1981) prepared amorphous silica particles according to Stöber's method and esterified the surface silanol groups of the electrostatically stabilized particle with octadecyl alcohol, which rendered the particle lyophilic and readily dispersible in nonpolar (organic) solvents. More recently, Lee and Yang (1998a) considered the stabilization effects for two different silane coupling agents, vinyltriethoxy silane (VTES) and γ-methacryloxypropyl triethoxy silane (MPTES). Through the sol–gel method via hydrolysis and condensation of silicon alkoxide, tetraethylorthosilicate (TEOS), monodisperse silica particles were synthesized for the dispersed phase. The monodisperse silica particles were stabilized with a silane coupling agent and used for the preparation of hard sphere dispersion for both rheological and rheo-optical measurements. The van der Waals dispersion forces between the particles suspended in a refractive-index matching solvent, for example, cyclohexane or tetrahydrofurfuryl alcohol, were shown to be negligible (Jansen, de Kruif, & Vrij, 1986). Consequently, the particles behaved like 'hard' spheres. Then, the rheological responses of the silica suspensions under simple shear flow were examined as functions of the particle size and volume fraction. In addition, we

examined flow-induced dichroism and order–disorder transition such as disappearance of hexagonally ordered layered structure and formation of particle clustering, which is responsible for the shear thickening.

2. Experimental

2.1. Preparation of hard sphere silica suspension

Monodisperse silica particles were synthesized through the sol–gel method proposed by Stöber et al. (1968). Tetraethylorthosilicate (TEOS; $Si(OC_2H_5)_4$, Aldrich) and deionized water were used as reactants in ethanol medium (EP grade, Oriental Chemical). In order to obtain the spherical silica particles, ammonium hydroxide (Aldrich) was used as a morphological catalyst. The particle size was controlled by varying water content, and the solid content and monodispersity were enhanced by step-wise growth of the Stöber's particles as seeds, i.e. by sequentially adding TEOS at 12 h time intervals (Bogush et al., 1988; Oh et al., 1999). Detailed compositions of the reactants, particle size and BET surface area were summarized in Table 1. The silica particles synthesized by the multistep and single-step growth methods from the seed particles were designated by S2A3 and S5A1, respectively. The particle shape and size including its distribution were examined by transmission electron microscopy (EM912, Car Zeiss).

To screen the van der Waals attraction and at the same time, to render the suspension transparent for rheo-optical measurement, tetrahydrofurfuryl alcohol (THFFA, Aldrich) was used as a refractive-index ($n_D = 1.45$) matching solvent. Moreover, in order to remove any residual interparticle interaction, a silane coupling agent, 3-(trimethoxysilyl)propyl methacrylate (MPTS; $(CH_3O)_3Si(CH_2)_3OCOC(CH_3)$–$CH_2$, Aldrich) was coated on the silica particles by chemical adsorption before the particles were dispersed in the refractive-index matching solvent. MPTS was added to the final silica sol solution to ensure particle stability, and then the final molar concentration of MPTS in the sol solution was estimated to be [MPTS] = 0.1 M. The amount of MPTS adsorbed onto the silica particle was determined by measuring the concentration of free MPTS in the supernatant using a UV spectrometer at 270 nm. In summary, the final stock solution was prepared by multistep procedures; namely, synthesis of the monodisperse silica particles, MPTS coating, and evaporation of alcohol and the residual reactants. By doing this, we were able to prepare effectively 'hard sphere' suspensions.

In the present work, purification of the silica particles was a very important step since destabilization of the suspension was caused mainly by the residual water and unreacted silane coupling agent. Therefore, the synthesized silica particles were purified more than six times by successively adding high purity ethanol (GR grade, Merck) and removing the supernatant after each ultracentrifugation. The stock solutions of the purified silica were used to prepare the final monodisperse silica suspensions with various volume fractions. The final suspension was obtained by thoroughly mixing THFFA and silica stock solution and by evaporating the ethanol. The density of the suspended silica particle can be determined from the intrinsic viscosity of the monodisperse spherical suspension at extreme dilutions. Finally, the particle volume fraction was varied from 0.45 to 0.55.

2.2. Apparatus

The rheological behaviour was investigated with a HAAKE viscometer under steady shear flow using Couette geometry. Temperature was adjusted to 25°C for all measurements. Flow-induced dichroism of the concentrated suspensions was also investigated through two different optical alignments originally designed by Johnson, Frattini, and Fuller (1985). The optical arrangements were composed of a He–Ne laser (L; $\lambda = 632.8$ nm), a polarizer (P; 0°), an analyzer (A; 0°), two (or single) quarter wave plate(s) (QWP; 0°), a photoelastic modulator (PEM; 45°) and a photodiode detector (D). The phase modulation was designed to generate a sinusoidally modulated retardance of $\delta_m = A\sin(\omega t)$, in which a reference frequency ω was 50.3 kHz. The amplitude A was measured as $A = 506$ from $J_0(A) = 0$ through the blank test. The optical alignment for the flow-induced

Table 1
Compositions of the reactants in the step-wise growth reaction, mean radius and BET surface area of the model silica particles

	Seed composition	1st growth	2nd growth	3rd growth	Mean radius	BET surface area
S2A3	[TEOS] = 0.57 M [NH_3] = 0.71 M [H_2O] = 1.7 M	[TEOS] = 0.57 M	[TEOS] = 0.57 M	[TEOS] = 0.57 M	129.93 ± 9.30 nm	13.04 m^2/g
S5A1	[TEOS] = 0.57 M [NH_3] = 0.71 M [H_2O] = 5.0 M	[TEOS] = 0.57 M	—	—	272.78 ± 1.97 nm	5.966 m^2/g

dichroism consisted of L-PEM-QWP-sample-D. In this alignment, the ratio I/I_0 of the resultant intensity I to the initial intensity I_0 can be expressed in terms of the harmonic oscillations with the decoupled amplitude functions I_{dc}, $I_{1\omega}$ and $I_{2\omega}$ of zeroth, first and second harmonics. Also, the calibration constants $J_0(A)$, $J_1(A)$, and $J_2(A)$ of the optical analysis were determined for the optical trains of L-PEM-QWP-QWP-QWP-A-D following the standard procedures (Johnson et al., 1985; Kim, Yang, & Kim, 1997; Lee & Yang, 1998a; Lee et al., 1999). The result gave the ratio of $J_1/J_2 = 1.198$, which was very close to the theoretical value of 1.2. Then, the reduced dichroism (δ'') and orientation angle (χ^2) of a given sample in the shear flow field were determined by taking the Fourier transformation on the signals detected by a photodiode. From the reduced dichroism of a given sample for the light signal of wavelength λ, the flow-induced dichroism ($\Delta n''$) of the sample can be determined as $\Delta n'' = \delta''\lambda/2\pi d$ in which d is the optical path length through the sample. All the suspensions were loaded on a cone-and-plate flow cell with the cone angle of 2° and the optical path length d of 0.52 nm. The cone-and-plate flow cell was made of quartz glass in order to pass the He–Ne laser beam effectively. Uniform shear field was generated within the cone-and-plate geometry with the aid of a computer-controlled step-motor. The laser beam passed through the flow-gradient direction to probe the microstructure evolution as in the SANS observation by Laun et al. (1992).

3. Results and discussions

3.1. Characterization of the synthesized silica particles

The synthesized monodisperse silica particles were spherical and the average particle radii of S2A3 and S5A1 were 129.93 ± 9.30 nm and 272.78 ± 1.97 nm, respectively. TEM images of these silica particles are given in Fig. 1. In order to prepare the 'hard sphere' silica suspensions at various concentrations, the density of the suspended silica particle needs to be determined. Spherical particle density can be determined from the intrinsic viscosity of suspension at extreme dilutions. We measured the shear viscosity of extremely dilute suspensions using Ubbelohde capillary viscometer. The relative viscosity was plotted as a function of the particle volume fraction for smaller and larger particle suspensions as shown in Fig. 2. According to Einstein's theory, the intrinsic viscosity should be 5/2 for a spherical particle suspension. By fitting the viscosity data at extremely dilute concentrations to Einstein's theory, the density of the prepared silica particles was determined as 1.65×10^{-3} kg/m^3, 1.70×10^{-3} kg/m^3 for S2A3 and S5A1, respectively. These values of the particle density were very close to the previous results (Philipse & Vrij, 1989; Bender & Wagner, 1995; Lee et al., 1999). It is also noteworthy that deviations from Einstein theory occurred as the particle loading increased and the viscosity became more accurately predicted by Batchelor's higher order corrections, which reflects the interactions between two neighboring particles. Finally, the silica suspensions at various particle volume fractions $\phi = 0.45$, 0.50 and 0.55 could be prepared in THFFA solvent with a measured density.

Although a refractive-index matching solvent, tetrahydrofurfuryl alcohol (THFFA), was used to screen the van der Waals attraction, it was expected that there still remained residual interactions between the silica particles. To remove the residual interactions and thereby impart nearly 'hard sphere' characteristics, the silane coupling agent, MPTS was coated on the silica particle by chemical adsorption. To confirm the adsorption of MPTS onto the silica particles, the adsorbed amount of MPTS was measured by monitoring the concentration of free MPTS in the supernatant using UV spectrometer at 270 nm after centrifugation of the mixture of MPTS and stock silica particle suspension. The results in which the adsorption isotherms were fitted with Langmuir-type

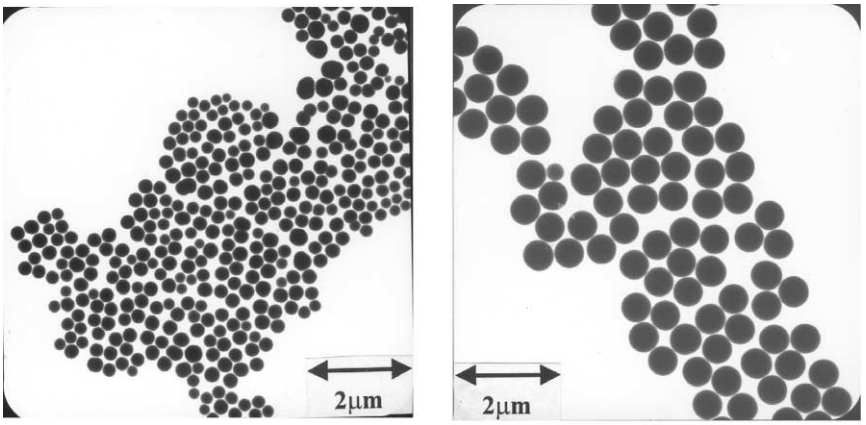

Fig. 1. TEM images of the prepared silica particles. (a) for particles S2A3; (b) for particles S5A1.

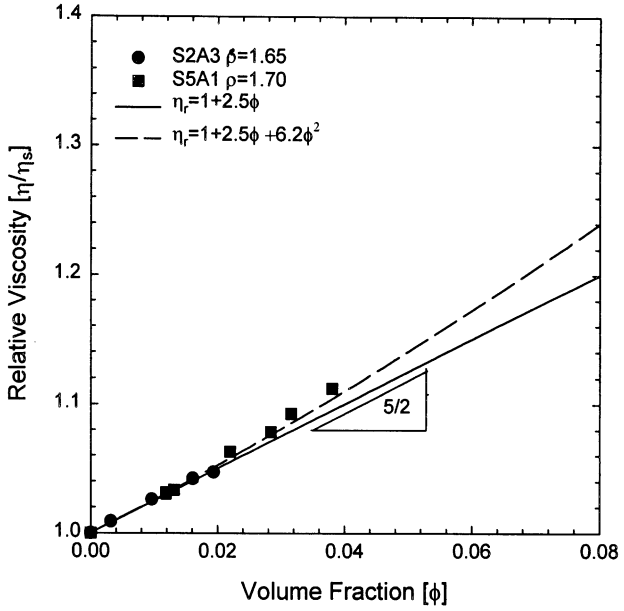

Fig. 2. Relative viscosity of the silica suspension as a function of the volume fraction at low concentrations. The particles were dispersed in the refractive-index matching solvent, THFFA.

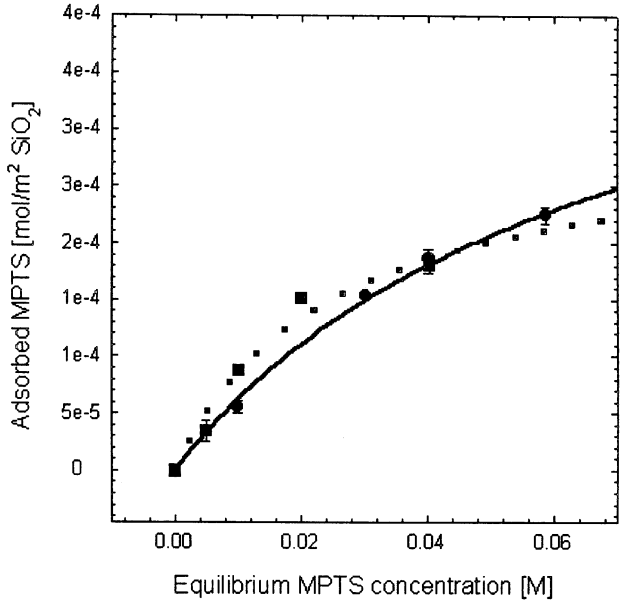

Fig. 3. Adsorption isotherms of MPTS onto the silica particles (solid line for particle S2A3; dotted line for particle S5A1).

adsorption equation are reproduced in Fig. 3. Although the size difference was considerable between particles S2A3 and S5A1, they showed similar adsorption behaviour. It should be noted that the adsorbed amount of MPTS onto the silica particles was small compared to its bulk concentration. Therefore, the particle purification was very important step and the synthesized silica particles must be purified more than six times by successively adding high-purity solvent and removing the supernatant after each ultra-centrifugation.

An appreciable size change was not observed by TEM and dynamic light scattering (DLS, Brookhaven Instrument) after the MPTS adsorption onto the silica surface, implying that the coated layer would be negligibly thin compared with the primary particle size. In addition, we measured the electrophoretic mobility of the MPTS coated silica particles with a zeta potential analyzer (Zeta Plus, Brookhaven). However, the zeta potential of the MPTS coated silica particle was too low to measure using the electrophoretic mobility in our Brookhaven instrument.

3.2. Rheological behaviour and dispersion stability

Significant deviations from Newtonian behaviour were induced by the combined contributions from the hydrodynamic and non-hydrodynamic interparticle interactions and random Brownian motions under a uniform shear field. It can be simply expected that increments of the particle content decrease the interparticle distance, and consequently lead to considerable changes in the flow properties of the suspension. Thus, rheological behaviour of the concentrated suspensions may be very complicated compared to other homogeneous fluids. In Fig. 4(a), the suspension viscosity was plotted as a function of the shear rate for two different volume fractions of $\phi = 0.50$ and 0.55. In this plot, the suspension consisted of the smaller particles S2A3, which were stabilized with MPTS. The shear viscosity of the non-stabilized S2A3 particle suspensions was included in Fig. 4(b). As noted, a very severe shear thinning was observed in both Figs. 4(a) and (b). The effects of stabilization with MPTS could be identified from these rheological results. As shown in Fig. 4(b) for the smaller particle (S2A3) suspensions, a weak shear thickening was observed at $\phi = 0.55$ when they were not stabilized with MPTS. Meanwhile, the non-stabilized S2A3 particle suspension did not exhibit shear thickening up to the shear rate $\dot{\gamma} = 1000\,\mathrm{s}^{-1}$ at a slightly lower particle loading, $\phi = 0.50$. On the other hand, the S2A3 suspensions stabilized with MPTS showed smooth shear thinning behaviour without displaying shear thickening within our shear rate window at both $\phi = 0.50$ and 0.55, see Fig. 4(a).

The stabilization effects were pronounced for the larger particle (S5A1) suspension as shown in Figs. 5(a) and (b). For the suspension of particles S5A1 stabilized with MPTS, the shear viscosity shear thinned smoothly without experiencing shear thickening at $\phi = 0.45$. It can be noted from Fig. 5(a) that when the volume fraction exceeded 0.50, the stabilized suspension of S5A1 particles experienced abrupt shear thickening. However, for the non-stabilized suspension of S5A1, unstable flow behaviour was observed and the shear thickening occurred at

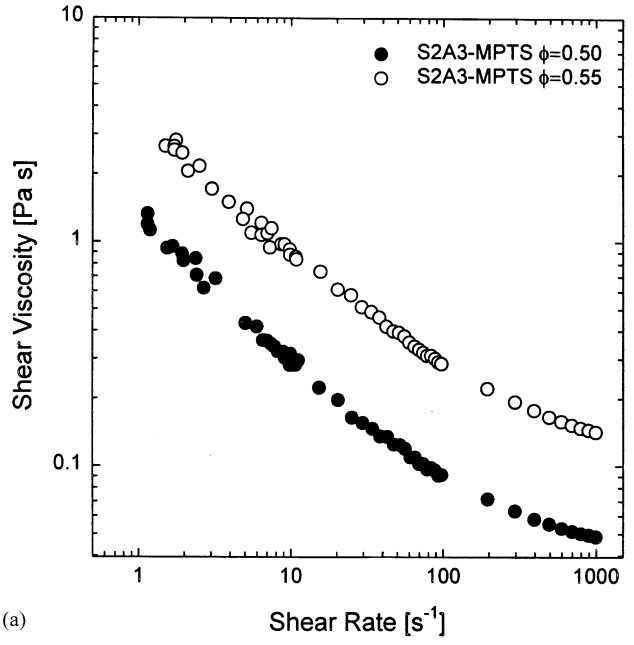

(a)

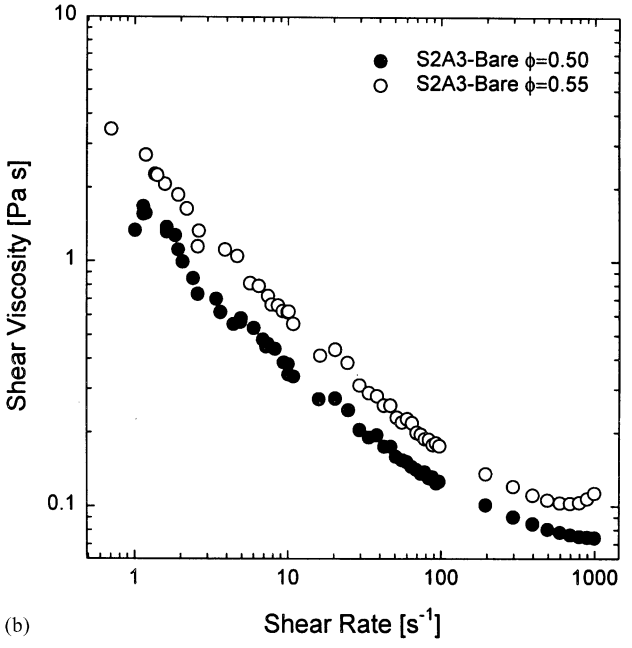

(b)

Fig. 4. Shear viscosity of a concentrated suspension as a function of the shear rate. Silica particles, S2A3, were loaded up to either $\phi = 0.50$ or 0.55 at 25°C. (a) for the particles stabilized with MPTs; (b) for the bare silica particles. Shear thickening was only observed at steady shear rate sweep for the suspensions of non-stabilized particles, S2A3, at $\phi = 0.55$.

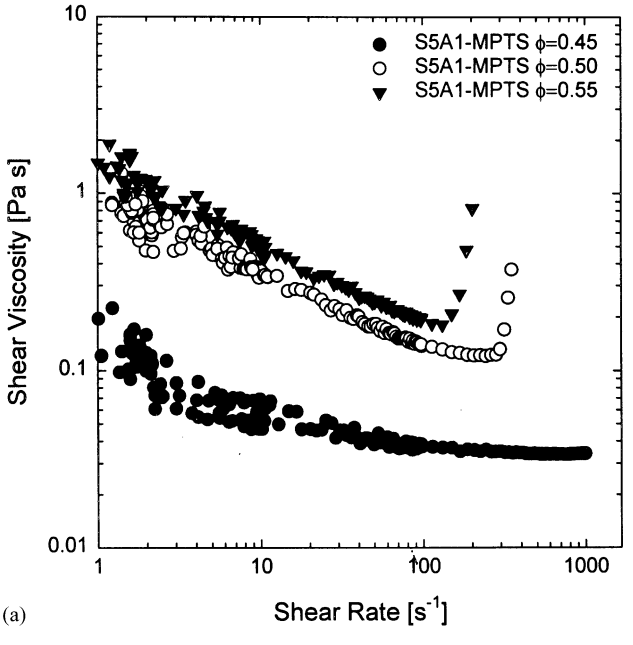

(a)

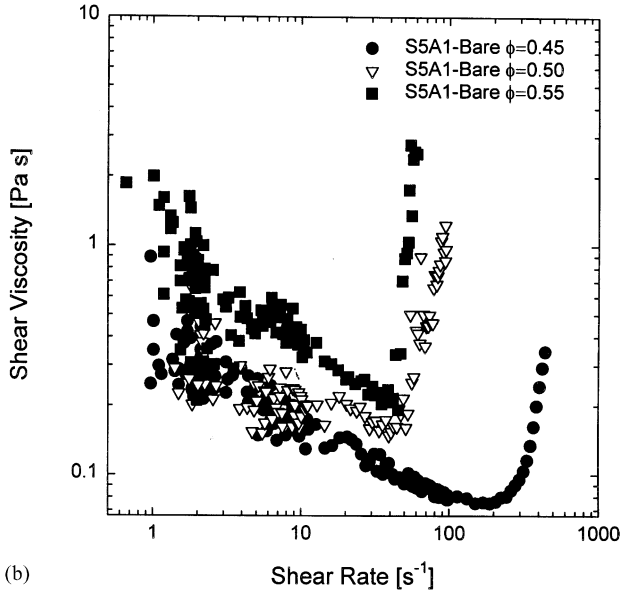

(b)

Fig. 5. Shear viscosity of a concentrated suspension as a function of the shear rate. Particles, S5A1, were loaded up to $\phi = 0.45, 0.50$ or 0.55 at 25°C. (a) for the particles stabilized with MPTS; (b) for the bare silica particles.

volume fractions ϕ above 0.45, see Fig. 5(b). Moreover, the steric stabilization with MPTS retarded the onset of shear thickening, i.e., the shear thickening occurred at a higher shear rate for the stabilized suspension than it would do for the non-stabilized suspension.

The so-called Stokesian dynamics simulation shows that Brownian contribution to the shear stress diminishes leaving only the hydrodynamic contribution as the shear rate increases. The disappearance of the Brownian contribution leads to a viscosity reduction, i.e., shear thinning since the Brownian fluctuations tend to form a random disordered structure. It is also obvious that the Brownian contribution to a suspension of the smaller particles can be sustained at the higher shear rates. In addition, at a given volume fraction, the interparticle interaction becomes stronger for smaller particle suspension due to closer inter-particle distance. Thus, for a given particle volume fraction, the suspension of

smaller particles S2A3 possesses higher viscosity at low shear rates. Moreover, the onset of shear thickening appeared at much higher shear rates for the smaller particle suspension due to the pronounced Brownian thermal agitation.

3.3. Rheo-optical responses and the origin of shear thickening

In the previous section, we monitored the stabilization effects of MPTS for the concentrated silica suspension rheologically. In this section, we consider the microstructural transition in concentrated particle suspension by measuring the flow-induced dichroism using an optical apparatus described previously. Recent advances in the optical techniques enable us to measure directly the optical anisotropic properties such as dichroism and birefringence of particle suspensions. When dispersed particles are subjected to an external flow, their microstructure is inevitably changed by the imposed flow. The structural anisotropy induced by flow will in turn create the optical anisotropy. Especially, the optical experiments make it possible to obtain the information about microstructural responses of materials in very short length scales. The merits of rheo-optical approach are direct reflection of molecular orientation and shape, spatial resolution within samples, high sensitivity, short time-scale response and correlation to rheological model (D'Haene, Mewis, & Fuller, 1993; Bender & Wagner, 1995). These merits lead to enormous rheo-optical studies of suspension, emulsion, polymer systems and surfactant system (D'Haene et al., 1993; Bender & Wagner, 1995; Johnson et al., 1985; Kishbaugh & McHugh, 1993; Lee & Yang, 1997; Lee & Yang, 1998a; Lee et al., 1999; Kim & Yang, 1997). In particular, on-site information on the flow-induced microstructure evolution under shear flow can be obtained from the rheo-optical measurement. Furthermore, these observations can be correlated directly to the macroscopic rheological properties. As mentioned earlier, S2A3 particles have somewhat broad size distribution and ordering does not occur even at high volume fractions. On the other hand, S5A1 particles have uniform size distribution and more likely to crystallize at the transition volume fraction of $\phi = 0.49$. Therefore, in the present study, we used only S5A1 particles to investigate the microstructure and phase transition with rheo-optical measurement.

In Fig. 6, the negative of flow-induced dichroism ($-\Delta n''$) of the stabilized and non-stabilized suspensions of the larger particles S5A1 was illustrated as a function of the shear rate at the particle loading $\phi = 0.45$. At low shear rates, the flow-induced dichroism was positive for the non-stabilized suspension. The positiveness of flow-induced dichroism was indicative of the fact that the non-stabilized particles formed weak aggregates at equilibrium and the aggregate structure was sustained under

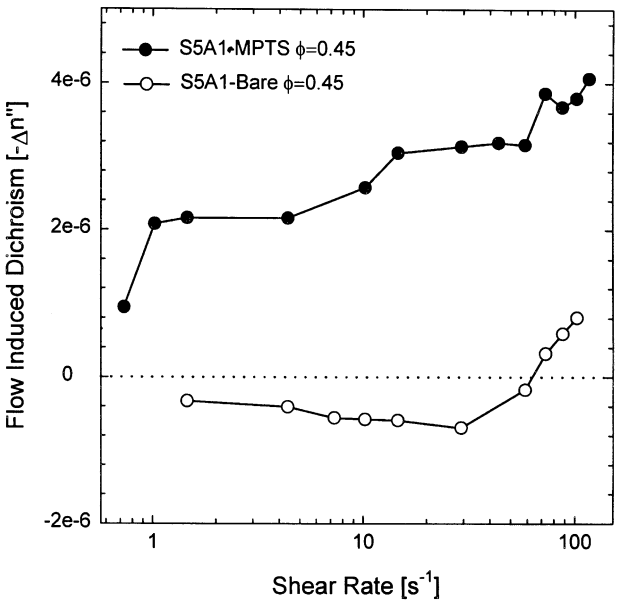

Fig. 6. Flow-induced dichroism as a function of the shear rate. Particles, S5A1, were either stabilized by the steric layer of MPTS or non-stabilized and loaded up to $\phi = 0.45$.

a weak flow. As expected, the flow-induced dichroism underwent sign change at high shear rate of about 60 s^{-1}. The sign change in the flow-induced dichroism of the non-stabilized suspension could be explained by considering that the micro-phase domain or the particle aggregates, which were present at low shear rates, were broken up as the shear rate increased. On the other hand, in case of the stabilized S5A1 suspension, the flow-induced dichroism showed no sign change and increased monotonically with shear rate. The monotonic increase in the flow-induced dichroism for the suspension stabilized by the steric layer of MPTS indicated that the ordered layers or strings of particles were aligned to the flow direction. The present result of flow-induced dichroism of $\phi = 0.45$ is somewhat contradictory to the recent simulation results (Foss & Brady, 2000; Catherall et al., 2000), which predicted no flow-induced ordering. As mentioned earlier, the zeta-potential of the silica particles was too low to measure using our electrophoresis apparatus. However, there might still exist residual surface charges as noted in the previous reports (Bender & Wagner, 1995; Lee et al., 1999). Therefore, the observed flow-induced dichroism for $\phi = 0.45$ may be caused by local formation of layered or string structure due to residual charge on the particle surface.

From now on, we consider highly concentrated silica suspensions of $\phi = 0.50$ and 0.55, in which the steric stabilization is expected to play an important role in the microstructural transitions and rheological responses. As mentioned earlier, when the recombination of particles under flow is ultimately restricted by strong interactions between the ordered layers of strings aligned to the flow

direction, the increased lubrication stress between the nearby particles is transferred to the medium solvent (Hoffman, 1972, 1974; Barnes et al., 1989; Boersma et al., 1990a,b; Laun et al., 1992; D'Haene et al., 1993; Bender & Wagner, 1996; Lee & Yang, 1998b). Hoffman (1972) showed the distinct ordered diffraction pattern of hexagonal crystal structure at shear thinning, and later the disordered diffraction form of amorphous materials after shear thickening. Meanwhile, Stokesian dynamics simulation (Brady, 1989; Bossis & Brady, 1993; Brady & Morris, 1997) suggested that the shear thickening may be induced by the cluster formation due to extremely strong hydrodynamic force of a particulate suspension.

To examine the basic thrust of shear thickening of concentrated hard sphere suspension, we observed the shear-induced dichroism of the concentrated suspensions of S5A1 stabilized with MPTS. The suspensions considered here are highly concentrated and the particle loadings are as high as $\phi = 0.50$ and 0.55. Figs. 7(a) and (b) displayed the direct correlation between the flow-induced dichroism and the shear viscosity as a function of the shear rate. For highly concentrated suspensions of $\phi = 0.50$ and 0.55, the flow-induced dichroism increases with shear rate in the weak flow regime, then appears to pass through a maximum and decreases rapidly at high shear rates as shown in Figs. 7(a) and (b). This clearly shows that highly concentrated suspensions undergo the order–disorder transition by an imposed shear flow and well coincides our previous report, in which hard sphere silica suspensions particles were stabilized MPTES (Lee et al., 1999).

We now consider in detail the origin of shear thickening in view of the flow-induced microstructure. Even at equilibrium state, ideal hard spheres begin to form an ordered structure above the melting volume fraction, ϕ_m, purely by entropic process. In particular, when $0.5 < \phi < 0.55$, the random disordered structures and the colloidal crystalline structure coexist and the formation of face centered cubic (FCC) or hexagonal closed packing (HCP) colloidal crystalline structure is completed when ϕ exceeds 0.55. In the present study, we considered highly concentrated suspensions with the particle volume fractions in the range of $0.5 < \phi < 0.55$, and the particles formed an ordered structure in the absence of flow. The shear thinning observed at high concentrations in this study arises from those ordered crystalline structures. When ordered phase is forced to flow, macrocrystalline structure deforms and the direction of closest packing of the spheres is aligned to flow velocity, while the planes containing the closest packings are parallel to the shearing surface (Ackerson, 1990; Larson, 1999). Thus, at low shear rates, the three-dimensionally ordered structure transforms into a two-dimensionally layered structure, which permits continuous deformation. For FCC structure under shear flow, the closest packing direction is 110 parallel to the flow velocity, while the

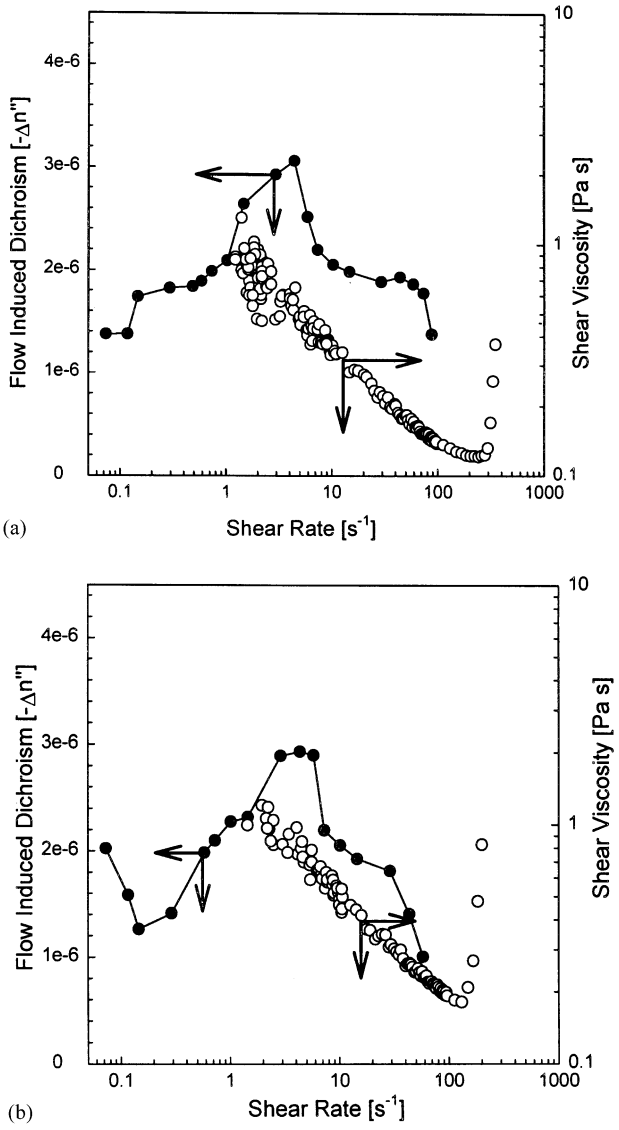

Fig. 7. Flow-induced dichroism and shear viscosity as a function of the shear rate. Particles, S5A1, were stabilized by the steric layer of MPTS at 25°C. (a) for $\phi = 0.50$; (b) for $\phi = 0.55$.

slipping planes parallel to the rheometer walls are 111 planes. In this orientation, particles in slipping planes (i.e., 111 planes of FCC) are in a two-dimensional hexagonal arrangement. Under these circumstances, the spacing between spheres in the gradient direction is maximized, and the spheres of hexagonally ordered layers can then most readily move over one another. Indeed, at low shear rates, the magnitude of flow-induced dichroism detected from the suspension with $\phi = 0.55$ decreased with increase of the shear rate up to 0.1 s^{-1}, see Fig. 7(b). This decrease in dichroism at extremely low shear rates was caused by the microstructural phase transition from 3-D ordered structure to 2-D layered structure. Meanwhile, for $\phi = 0.50$ at which the ordering begins to occur, transformation from 3-D to 2-D

structure at low shear rates cannot be detected from our rheo-optical measurement. This is because complete 3-D crystallization cannot be formed completely in suspensions with $\phi = 0.50$.

Recently, Stokesian dynamics simulation of Foss and Brady (2000) showed that although no flow-induced ordering occurs in hard sphere suspensions with $\phi < 0.49$, hexagonally packed string ordering occurs with $\phi = 0.49$. This is clearly consistent with the present results. Under these circumstances, i.e., when 2-D ordered structure develops, dichroism increases monotonically and reaches a maximum as the shear rate increases, see Figs. 7(a) and (b). After passing the maximum point, dichroism decreases monotonically and falls and vanishes asymptotically prior to shear thickening. The decrease in dichroism is caused by order-to-disorder transition, i.e., the breakup of 2-D ordered layer before shear thickening. It is noteworthy that the suspensions at high shear rates near the onset of shear thickening became turbid and scattered the light so severely that the detected dichroism signal was not reproducible. The flow-induced turbidity may arise from the formation of relatively large particle clusters and occurs often in other heterogeneous systems such as block copolymers, concentrated polymer solutions and nonstabilized suspensions (Lee et al., 1999).

The present results coincide also with the previous report of Laun et al. (1992), but seem contrary to the previous report of D'Haene et al. (1993) or Bender and Wagner (1995), who could not observe ordering in shear thickening suspensions. As summarized in Table 2, our optical system is different from that of D'Haene et al. (1993) or Bender and Wagner (1995), and laser beam in our system passed through the flow-gradient direction as in the SANS observation by Laun et al. (1992) to probe the microstructure evolution. This is because the flow-induced dichroism from light passed in the flow-gradient direction probes the order–disorder transition most effectively for highly concentrated particle suspensions, such as disappearance of hexagonally ordered layered structure and formation of particle clustering. Meanwhile, laser beams of D'Haene et al. (1993) and Bender and Wagner (1995) passed in the vorticity direction.

In fact, dichroism experiments alone can hardly provide clear evidence that an order-to-disorder transition has occurred. However, our dichroism and shear viscosity behavior were consistent with other scattering results of Laun et al., which clearly confirmed the order–disorder transition. The SANS patterns show that the breakup of the hexagonally ordered layers begins at shear rates lower than the onset of shear thickening. This is also consistent with our flow-dichroism result in that the reduction of flow-induced dichroism begins before the onset of shear thickening. Thus, the breakup of a hexagonally ordered layered structure appears to be an insufficient condition for shear thickening. The so-called Stokesian dynamics simulation of Brady (1993) showed that the stresses in shear thickening suspensions are predominantly hydrodynamic in origin and are due to particle clustering. The particle clustering produces effectively elongated aggregates and increases viscous dissipation significantly. Thus, the shear thickening requires not only that the sliding layers be broken down by shear, but that the fragment of these layers must collide with each other to form structures whose average dimensions in the flow-gradient direction are large. Such structure can jam the flow, leading to abrupt shear thickening (Chow & Zukoski, 1995a). Meanwhile, if the particle concentration is not high enough, layer breakdown does not lead to jamming, and there is no abrupt shear thickening. Overall, the general features of order–disorder transition and subsequent shear thickening observed through a rather simple rheo-optical instrument are consistent with sophisticated SANS images.

4. Summary

In the present paper, the monodisperse silica suspensions were prepared by sol–gel method and

Table 2
Methods of observation of the microstructure evolution and beam directions through flow cell

Author	Type of particle	Microstructural evolution method	Probed direction
Ackerson (1990)	Sterically stabilized PMMA	Light scattering	Velocity gradient direction
Laun et al. (1992)	Charge-stabilized styrene-ethylacrylate-copolymer sphere	SANS	Velocity gradient direction
D'Haene et al. (1993)	Sterically stabilized PMMA	Optical method	Vorticity direction
Chen et al. (1994)	Charge-stabilized styrene latex	SANS	Velocity gradient direction
Bender and Wagner (1995)	Sterically stabilized silica	Optical method	Vorticity direction
Lee et al. (1999)	Sterically stabilized silica	Optical method	Velocity gradient direction

their rheological behaviour and phase stability were investigated experimentally. In particular, the stabilization effects of a silane coupling agent of MPTS and the shear thickening of highly concentrated suspensions were studied. The conclusions from the present investigations are as follows;

1. Flow-induced microstructure was detected effectively by the rheological and optical measurements. For the untreated bare particle suspension, the micro-phase domains or the particle aggregates that were present at low shear rates were broken up as the shear rate increased. The silane coupling agent, MPTS, was effective in enhancing the suspension stability and gave rise to effective steric repulsion between the particles even in concentrated suspensions.

2. Highly concentrated suspensions undergo a transition from rapid shear thinning to shear thickening. The rapid shear thinning at low shear rates indicates the formation of three-dimensional macrocrystalline structure of FCC or HCP at high volume fractions. For suspension of the larger particles S5A1, the shear thickening occurs for $\phi \geqslant 0.50$. On the other hand, the shear thickening does not develop in the suspension of the stabilized smaller particles S2A3 even at $\phi = 0.55$ due to the deficiency of hydrodynamic force. In addition, the non-stabilized suspension experiences the shear thickening at a relatively low shear rate compared with the stabilized suspension of identical volume fraction. This is because the particle clusters are formed with ease in the non-stabilized suspension under high shear rates due to the weak interparticle interactions.

3. For highly concentrated suspensions, the intensity of flow-dichroism measured through the flow-gradient direction increases with shear rate in the weak flow regime, then appears to pass through a maximum and decreases at high shear rates. This clearly shows that highly concentrated suspensions experience the order–disorder transition by an imposed shear flow. Specifically, the flow-induced dichroism suggests that ordering of the particle suspension be reduced gradually before the onset of shear thickening. This implies that the shear thickening develops after the order–disorder transition fully proceeds. On the other hand, for moderately concentrated suspensions, the flow-dichroism increases monotonically with no indication of the order–disorder transition as the shear rate increases.

Acknowledgements

The authors wish to acknowledge support by KOSEF under Grant No. 1999-1-307-004-3. This work was also supported partly by the Brain Korea 21 project.

References

Ackerson, B. J. (1990). Shear induced order and shear processing of model hard sphere suspensions. *Journal of Rheology*, *34*, 553–590.

Barnes, H. A. (1989). Shear-thickening ('dilatancy') in suspensions of non-aggregating solid particles dispersed in Newtonian fluids. *Journal of Rheology*, *33*, 329–366.

Barnes, H. A., Hutton, J. F., & Walters, K. (1989). *An introduction to rheology*. New York: Elsevier Science Publishers.

Batchelor, G. K. (1977). The effect of Brownian motion on the bulk stress in a suspension of spherical particles. *Journal of Fluid Mechanics*, *83*, 97–117.

Bender, J. W., & Wagner, N. J. (1995). Optical measurement of the contributions of colloidal forces to the rheology of concentrated suspensions. *Journal of Colloid and Interface Science*, *172*, 171–184.

Bender, J., & Wagner, N. J. (1996). Reversible shear thickening in monodisperse and bidisperse colloidal dispersions. *Journal of Rheology*, *40*, 899–916.

Boersma, W. H., Baets, P. J. M., Laven, J., & Stein, H. N. (1990a). Time-dependent behavior and wall slip in concentrated shear thickening dispersions. *Journal of Rheology*, *35*, 1093–1120.

Boersma, W. H., Laven, J., & Stein, H. N. (1990b). Shear thickening (dilatancy) in concentrated dispersions. *A.I.Ch.E Journal*, *36*, 321–332.

Bogush, G. H., Tracy, M. A., & Zukoski, C. G. (1988). Preparation of monodisperse silica particles: Control of size and mass fraction. *Journal of Non-Crystalline Solids*, *104*, 95–106.

Bossis, G., & Brady, J. F. (1989). The rheology of Brownian suspensions. *Journal of Chemical Physics*, *91*, 1866–1874.

Brady, J. F. (1993). The rheological behavior of concentrated colloidal dispersions. *Journal of Chemical Physics*, *99*, 567–581.

Brady, J. F., & Morris, J. F. (1997). Microstructure of strongly sheared suspensions and its impact on rheology and diffusion. *Journal of Fluid Mechanics*, *348*, 103–139.

Catherall, A. A., Melrose, J. R., & Ball, R. C. (2000). Shear thickening and order–disorder effects in concentrated colloids at high shear rates. *Journal of Rheology*, *44*, 1–25.

Chen, L.B., Ackerson, B.J., & Zukoski, C.F. (1994). Rheological consequences of microstructural transitions in colloidal crystals. Journal of Rheology, 38, 1-25, 193–216.

Choi, G. N., & Krieger, I. M. (1986). Rheological studies on sterically stabilized model dispersions of uniform colloidal spheres II. Steady-shear viscosity. *Journal of Colloid and Interface Science*, *113*, 101–113.

Chow, M. K., & Zukoski, C. F. (1995a). Gap size and shear history dependencies in shear thickening of a suspension ordered at rest. *Journal of Rheology*, *39*, 15–32.

Chow, M. K., & Zukoski, C. F. (1995b). Nonequilibrium behavior of dense suspensions of uniform particles: Volume fraction and size dependence of rheology and microstructure. *Journal of Rheology*, *39*, 33–59.

D'Haene, P., Mewis, J., & Fuller, G. G. (1993). Scattering dichroism measurements of flow-induced structure of a shear thickening suspension. *Journal of Colloid and Interface Science*, *156*, 350–383.

de Kruif, C. G., van lersel, E. M. F., Vrij, A., & Russel, W. B. (1985). Hard sphere colloidal dispersion: Viscosity as a function of shear rate and volume fraction. *Journal of Chemical Physics*, *83*, 4717–4725.

Fagan, M. E., & Zukoski, C. F. (1997). The rheology of charge stabilized silica suspensions. *Journal of Rheology*, *41*, 373–397.

Foss, D. R., & Brady, J. F. (2000). Structure, diffusion and rheology of Brownian suspensions by Stokesian dynamics simulation. *Journal of Fluid Mechanics*, *407*, 167–200.

Furth, R., & Cowper, A. D. (1956). *Investigations on the theory of the Brownian movement by A. Einstein*. New York: Dover Publications Inc.

Gast, A. P., & Russel, W. B. (1998). Simple ordering in complex fluids. *Physics Today*, *51*(12), 24–30.

Graham, A. L., Steele, R. D., & Bird, R. B. (1984). Particle clusters in concentrated suspensions: 3. Prediction of suspension viscosity. *Industrial and Engineering Chemistry, Fundamentals*, *23*, 420–425.

Hoffman, R. L. (1972). Discontinuous and dilatant viscosity behavior in concentrated suspensions I. Observation of a flow instability. *Transactions of the Society of Rheology*, *16*, 155–173.

Hoffman, R. L. (1974). Discontinuous and dilatant viscosity behavior in concentrated suspensions II. Theory and experimental tests. *Journal of Colloid and Interface Science*, *46*, 491–506.

Jansen, J. W., de Kruif, C. G., & Vrij, A. (1986). Attraction in sterically stabilized silica dispersions. II Experiments on phase separation induced by temperature variation. *Journal of Colloid and Interface Science*, *114*, 481–504.

Johnson, S. J., Frattini, P. L., & Fuller, G. G. (1985). Simultaneous dichroism and birefringence measurements of dilute colloidal suspensions in transient shear flow. *Journal of Colloid and Interface Science*, *104*, 440–449.

Kim, W.-J., Yang, S.-M., & Kim, M. S. (1997). Additive effects on the microstructure evolution in hexadecyltrimethylammonium bromide solution and its rheological properties. *Journal of Colloid and Interface Science*, *194*, 108–119.

Kishbaugh, A. J., & McHugh, A. J. (1993). A rheo-optical study of shear-thickening and structure formation in polymer solutions. Part I. Experimental. *Rheologica Acta*, *32*, 9–24.

Krieger, I. M., & Dougherty, T. J. (1959). A mechanism for non-Newtonian flow in suspensions of rigid spheres. *Transactions of the Society of Rheology*, *3*, 137–152.

Larson, R. G. (1999). *The structure and rheology of complex fluids*. New York: Oxford University Press.

Laun, H. M., Bung, R., Hess, S., Loose, W., Hess, O., Hahn, K., Hadicke, E., Hingmann, R., Schmidt, F., & Lindner, P. (1992). Rheological and small angle neutron scattering investigation of shear-induced particle structures of concentrated polymer dispersions submitted to plane Poiseuille and Couette flow. *Journal of Rheology*, *36*, 743–787.

Lee, J.-D., So, J.-H., & Yang, S.-M. (1999). Rheological behavior and stability of concentrated silica suspensions. *Journal of Rheology*, *43*, 1117–1140.

Lee, J.-D., & Yang, S.-M. (1997). Rheo-optical behavior and microstructural changes in silica particle dispersions. *HWAHAKKONGHAK*, *35*, 782–790.

Lee, J.-D., & Yang, S.-M. (1998a). Rheo-optical behavior and stability of silica particle suspension coated with silane coupling agents. *Journal of Colloid and Interface Science*, *205*, 397–409.

Lee, J.-D., & Yang, S.-M. (1998b). Rheological behavior of concentrated silica particle suspensions prepared by sol-gel method. *Korean Journal of Rheology*, *10*, 24–30.

Oh, M.-H., So, J.-H., Lee, J.-D., & Yang, S.-M. (1999a). Preparation of silica dispersion and its phase stability in the presence of salts. *Korean Journal of Chemical Engineering*, *16*, 532–537.

Oh, M.-H., So, J.-H., Lee, J.-D., & Yang, S.-M. (1999b). Rheological evidence for the silica-meditated gelation of xanthan gurn. *Journal of Colloid and Interface Science*, *216*, 320–328.

Philipse, A. P., & Vrij, A. (1989). Preparation and properties of nonaqueous model dispersions of chemically modified, charged silica spheres. *Journal of Colloid and Interface Science*, *128*, 121–136.

Russel, W. B., & Gast, A. P. (1986). Nonequilibrium statistical mechanics of concentrated colloidal dispersion: Hard spheres in weak flows. *Journal of Chemical Physics*, *84*, 1815–1826.

Russel, W. B., Saville, D. A., & Schowalter, W. R. (1989). *Colloidal dispersion*. New York: Cambridge University Press.

Stöber, W., Fink, A., & Bohn, E. (1968). Controlled growth of monodisperse silica spheres in the micron size range. *Journal of Colloid and Interface Science*, *26*, 62–69.

van der Werff, J. C., & de Kruif, C. G. (1989). Hard-sphere colloidal dispersion: The scaling of rheological properties with particle size, volume fraction, and shear rate. *Journal of Rheology*, *33*, 421–454.

van Helden, A. K., Jansen, J. W., & Vrij, A. (1981). Preparation and characterization of spherical monodisperse silica dispersion in nonaqueous solvents. *Journal of Colloid and Interface Science*, *81*, 354–368.